BJR|Open https://doi.org/10.1259/bjro.20180023

Received: 29 August 2018 | Revised: 26 February 2019 | Accepted: 27 February 2019

Cite this article as:
Dong X, Chunrong Y, Hongjun H, Xuexi Z. Differentiating the lymph node metastasis of breast cancer through dynamic contrast-enhanced magnetic resonance imaging 2019; **1**: 20180023.

ORIGINAL RESEARCH

Differentiating the lymph node metastasis of breast cancer through dynamic contrast-enhanced magnetic resonance imaging

[1]XU DONG, [1]YU CHUNRONG, [1]HOU HONGJUN and [2]ZHANG XUEXI

[1]WeiHai Central Hospital, Weihai City, ShanDong, China
[2]GE Healthcare, Shanghai, China

Address correspondence to: Dr Zhang Xuexi
E-mail: *zxxsfm@163.com*

Objective: Lymph node metastasis is an important trait of breast cancer, and tumors with different lymph node statuses require various clinical treatments. This study was designed to evaluate the lymph node metastasis of breast cancer through pharmacokinetic and histogram analysis via dynamic contrast-enhanced (DCE) MRI.

Methods and materials: A retrospective analysis was conducted to quantitatively evaluate the lymph node statuses of patients with breast cancer. A total of 75 patients, i.e. 34 patients with lymph node metastasis and 41 patients without lymph node metastasis, were involved in this research. Of the patients with lymph node metastases, 19 had sentinel lymph node metastasis, and 15 had axillary lymph node metastasis. MRI was conducted using a 3.0 T imaging device. Segmentation was carried out on the regions of interest (ROIs) in breast tumors under DCE-MRI, and pharmacokinetic and histogram parameters were calculated from the same ROIs. Mann–Whitney *U* test was performed, and receiver operating characteristic curves for the parameters of the two groups were constructed to determine their diagnostic values.

Results: Pharmacokinetic parameters, including Ktrans, Kep, area under the curve of time–concentration, and time to peak, which were derived from the extended Tofts linear model for DCE-MRI, could highlight the tumor areas in the breast and reveal the increased perfusion. Conversely, the pharmacokinetic parameters showed no significant difference between the patients with and without lymph node metastases. By contrast, the parameters from the histogram analysis yielded promising results. The entropy of the ROIs exhibited the best diagnostic ability between patients with and without lymph node metastases ($p < 0.01$, area under the curve of receiver operating characteristic = 0.765, specificity = 0.706, sensitivity = 0.780).

Conclusion: In comparison with the pharmacokinetic parameters, the histogram analysis of the MR images could reveal the differences between patients with and without lymph node metastases. The entropy from the histogram indicated that the diagnostic ability was highly sensitive and specific.

Advances in knowledge: This research gave out a promising result on the differentiating lymph node metastases through histogram analysis on tumors in DCE-MR images. Histogram could reveal the tumors heterogenicity between patients with different lymph node status.

INTRODUCTION

Breast cancer is a highly common disease in females. It can be divided into several types based on histological or immunohistochemical examination; according to epidemiological data, females aged between 40 and 60 years are at a high risk of breast cancer.[1,2] Previous studies focused on differentiating benign and malignant breast tumors or grading malignant tumors through MRI, ultrasound, or mammography; with these techniques, the properties of breast tumors can be easily identified.

Lymph node metastasis is the most common form of tumor metastasis. In this state, tumor cells pass through the lymphatic wall and follow the lymph circulation into the lymph node. Lymph node metastasis is a frequent complication of breast cancer. Breast cancer cells undergoing lymph node metastasis initially pass through the sentinel lymph node and then transfer to the axillary lymph node. For patients with breast cancer, the higher the degree of lymph node metastasis is, the lower the cumulative survival rate is. In some special cases, lymph node metastasis may be detected during the first medical

examination of patients. The status of axillary lymph node metastasis is often regarded as an important indicator of prognosis for patients with breast cancer in clinical settings.[3,4]

MRI is a routine clinical examination to identify benign and malignant tumors in the breast. Pharmacokinetic parameters from dynamic contrast-enhanced (DCE) MRI can be obtained by simulating the time–concentration curves of contrast agents.[5] These parameters have been applied to predict the need for neoadjuvant chemotherapy[6] and radiation therapy.[7] Ktrans and other parameters describe the contrast agent washin and washout procedure and reflect the microstructural and microenvironmental changes inside tumors. Pharmacokinetic parameters have also been associated with biomarker and gene expression.[8]

The results of histogram analysis of MR images differ from those of pharmacokinetic analysis. Histograms focus on the distribution of pixel values in a region of interest (ROI). In breast cancer research, histograms have been used to clarify the difference between triple-negative breast cancer and ER-positive breast cancer.[9] Histograms from DCE-MRI can also be utilized to evaluate the response of patients with advanced breast cancer to neoadjuvant chemotherapy.[10] Histogram analysis has been performed to examine the parameters derived from a MR function sequence, and the histogram metrics of the perfusion fraction and pseudo-diffusivity of an intravoxel incoherent motion sequence are related to molecular prognostic factors and breast cancer malignancy.[11]

This research was designed to determine the biomarker that could reveal the differences in breast tumors with or without lymph node metastasis in terms of pharmacokinetic and histogram parameters.

METHODS AND MATERIALS

Patient selection

This research was approved by the ethics review boards of our hospital. 75 patients were finally involved in this research from June 2017 to March 2018. All of the lesions were confirmed through pathological examination, and DCE-MRI was performed before surgery or any other treatment was adopted. Informed consent was signed before the patients underwent DCE-MRI.

Of the 75 patients, 34 had lymph node metastases, namely, sentinel lymph node metastasis (19 patients) and axillary lymph node metastasis (15 patients). On the other hand, 34 patients with lymph node metastasis could also be divided into two groups, lymph node metastasis was found on the first biopsy in 21 patients, no lymph node metastasis was found in 13 other patients during the first biopsy, but subsequent lymph node metastasis was found. The data included in this study are taken from MR images that metastasis has been occurred.

Pathological examination showed that the pathological subtypes of the patients with breast cancer in the study included invasive breast cancer, papillary carcinoma, carcinoma mucosum, and ductal carcinoma *in situ*. No significant differences in age, tumor location (right or left), or genotyping were found between the patients with and without lymph node metastases. The detailed patient information is presented in Table 1.

Table 1. Patient information

Details		Lymph node metastasis (34)	No lymph node metastasis (41 patients)
Pathological types	Invasive breast cancer (Grade I)	15	10
	Invasive breast cancer (Grade II)	9	13
	Invasive breast cancer (Grade III)	7	8
	Papillary carcinoma	1	3
	Carcinoma mucosum	1	1
	Ductal carcinoma *in situ*	1	6
Sides	Left	19	21
	Right	16	20
Age	Age	54 ± 11	52.34 ± 11.6
Metastasis locations	Axillary lymph node metastasis	15	/
	Sentinel lymph node metastasis	19	/
Genotyping	Luminal A	8	13
	Luminal B	16	17
	Her2 positive	6	7
	Base like	3	4

MRI

MRI was conducted using a 3.0 T imaging device (Discovery MR 750, GE Healthcare, Milwaukee, WI) with an 8-channel breast phased array coil.

MR scanning included two sections, namely, unenhanced multi-flip angle (5°, 10°, and 15°) T_1 weighted imaging images, were collected initially using a vibrant sequence with only one phase to obtain the T_1 mapping. The details of the scan parameter was as follows: repetition time/echo time = 4.1/2.1 ms, flip angle = 5°/10°/15°, slice thickness = 6 mm, matrix size = 256 × 256 cm, number of slices = 80, and temporal resolution = 10 s. The field of view was adjusted for each patient. The images obtained through DCE-MRI were then collected using the vibrant sequence with the following parameters: repetition time/echo time = 4.1/2.1 ms, flip angle = 10°, slice thickness = 6 mm, matrix size 256 × 256 cm, and number of slices = 80. The field of view was also adjusted on the basis of the breast volume. The DCE-MRI sequence was completed within 5 min, and 30 phases were acquired. The total acquisition time of each patient was approximately 7–8 min.

Figure 1. Arterial input functions of the patients with breast cancer (a) and ROI segmentation on the largest cross-sectional slice on the tumor images (b). ROI, region of interest.

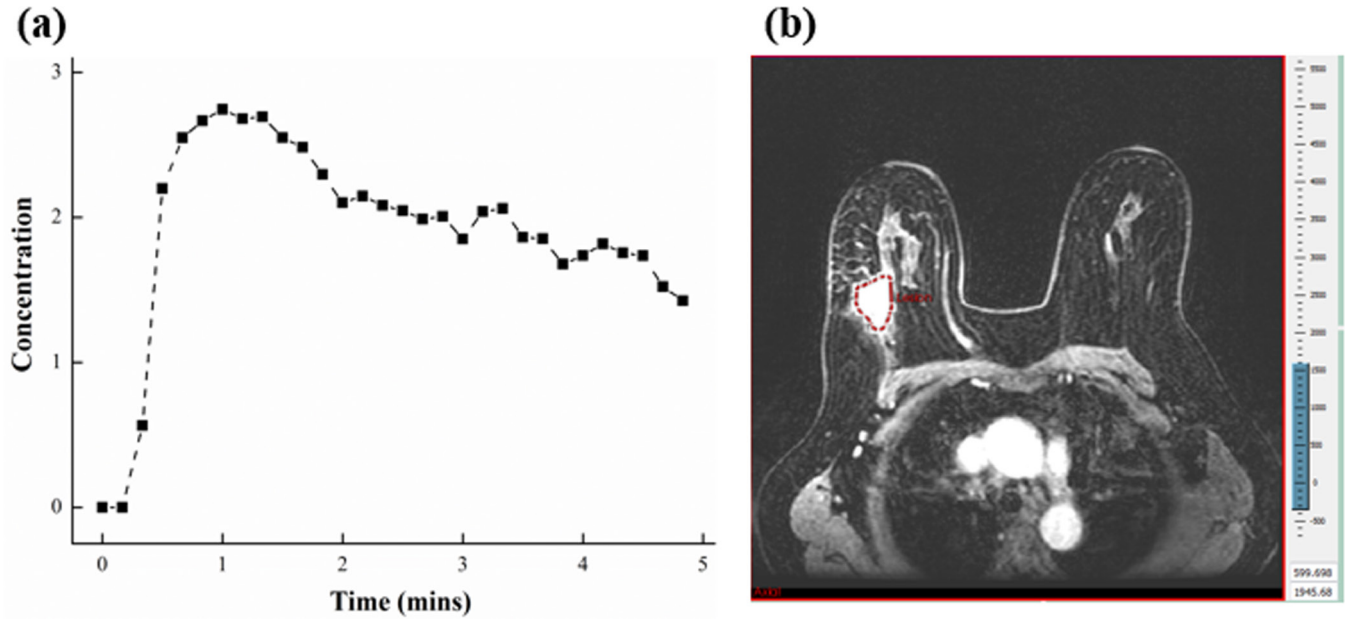

At the start of DCE-MRI, two unenhanced phases were initially collected, and 0.1 mmol/kg gadolinium contrast agent (Omniscan, GE Healthcare, Shanghai, China) was injected intravenously at a rate of 4 ml s^{-1}. Afterward, a 20 ml saline flush was injected through the antecubital vein.

Data processing

Data analysis was divided into two parts, namely, pharmacokinetic analysis and histogram analysis. Processing was achieved with Omini–Kinetic software (GE Healthcare, China, Shanghai). Pharmacokinetic parameters were calculated using an extended Tofts model,[12] and arterial input function was obtained by manually drawing a circle on the aorta pectoralis.

To obtain a clear tumor boundary, we drew one ROI for the breast tumor lesion on the phase corresponding to where the contrast agent concentration reached the maximum value as indicated by the arterial input function (Figure 1a). ROI

Figure 2. Pharmacokinetic (b) and histogram parameters (c) derived from ROIs in DCE-MRI (a) DCE-MRI,dynamic contrast-enhanced MRI; ROI, region of interest.

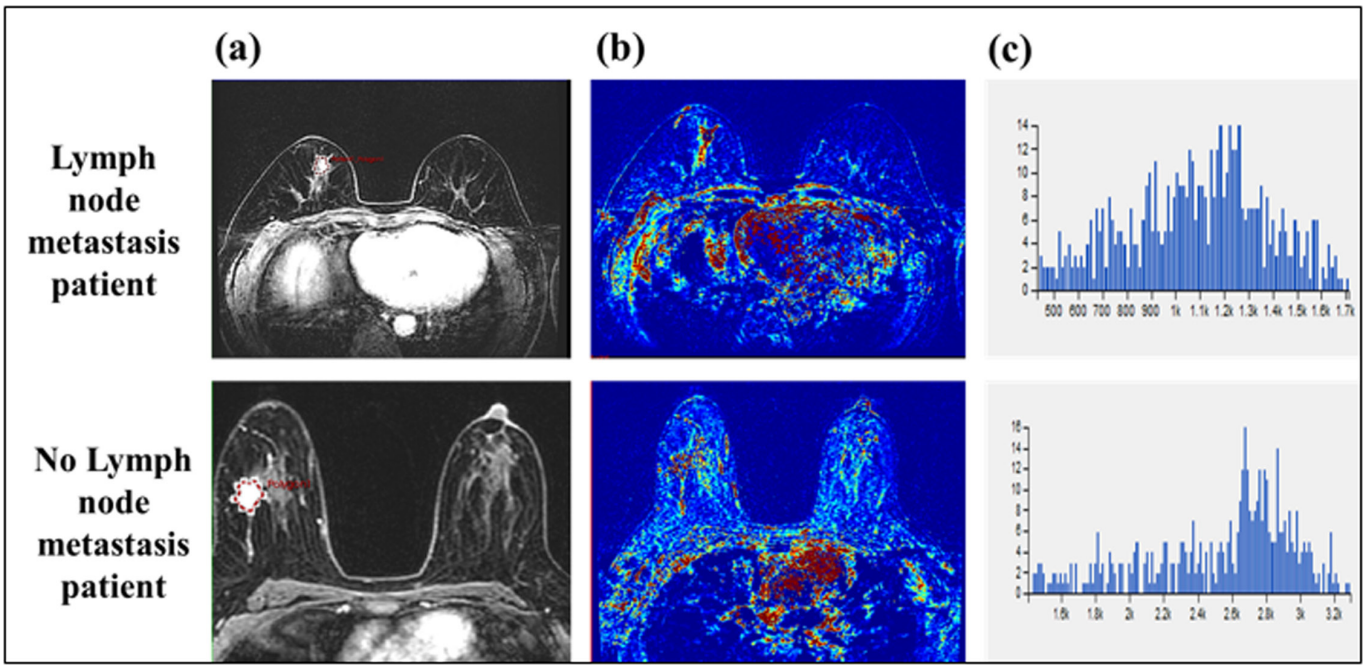

Table 2. Mann–Whitney *U* test of the pharmacokinetic parameters of patients with breast cancer with and without lymph node metastases ($\bar{x} \pm s$)

Pharmacokinetic parameters	Lymph node metastasis (34 patients)	No lymph node metastasis (41 patients)	Mann–Whitney *U* (*p* values)
Ktrans	0.209 ± 0.168	0.265 ± 0.262	0.551
Kep	0.966 ± 0.757	1.080 ± 0.759	0.580
AUC-TC	4.839 ± 2.774	5.157 ± 3.339	0.710
TTP	1.794 ± 0.482	1.81 ± 0.386	0.848

AUC-TC, area under the curve of the time–concentration curve; TTP, time to peak.

measurement was performed on the largest cross-sectional slice for the entire tumor images. A circle or a polygon was outlined around the tumors while avoiding the necrotic and vascular regions (Figure 1b). For each patient, the ROI size was 3–5 cm^2. The processing was finished by two radiologists with 7- and 10 year experiences, respectively. Disagreement between them was resolved by a consensus.

The pharmacokinetic and histogram parameters of the breast tumors were obtained from the same ROIs in DCE-MRI. In the pharmacokinetic parameter group, Ktrans, Kep, area under the curve (AUC) of the time–concentration curve (AUC-TC), and time to peak (TTP) were obtained for each patient. In the histogram analysis group, 13 parameters, namely, skewness, kurtosis, uniformity, energy, entropy, frequency size, quantile5, quantile10, quantile25, quantile50, quantile75, quantile90, and quantile95, were calculated from each patient.[13]

Statistical analysis

Statistical analysis was performed with IBM SPSS Statistics v. 19.0 (IBM, Chicago, IL). Mann–Whitney *U* test was performed, and receiver operating characteristic (ROC) curves were constructed for the pharmacokinetic and histogram parameters obtained from the patients with and without lymph node metastases. Differences at $p < 0.05$ were considered statistically significant. The AUCs of the ROC between 0.50 and 0.7, between 0.7 and 0.9, and higher than 0.9 indicated low, certain, and high accuracies, respectively. When the AUC of ROC ≤0.5, the diagnostic method was considered completely ineffective and had no diagnostic value.

Results

Figure 2(a) presents the segmentation of the images from DCE-MRI for the patients with and without lymph node metastases. Figure 2(b) reveals the pharmacokinetic maps of the whole slice. Figure 2(c) displays the histogram analysis of the ROI in Figure 2(a).

Table 2 shows the Mann–Whitney *U* test of Ktrans, Kep, AUC-TC, and TTP. No significant differences existed between the patients with and without lymph node metastases. The pharmacokinetic

Table 3. Mann–Whitney *U* test of the histogram parameters of patients with breast cancer with and without lymph node metastases ($\bar{x} \pm s$)

Histogram parameters	Lymph node metastasis (34 patients)	No lymph node metastasis (41 patients)	Mann–Whitney *U* (*p* values)
Skewness	−0.549 ± 0.646	−0.612 ± 0.783	0.924
Kurtosis	0.22 ± 1.500	0.271 ± 1.930	0.750
Uniformity	0.701 ± 0.122	0.711 ± 0.159	0.587
Energy	0.018 ± 0.012	0.042 ± 0.046	<0.01
Entropy	6.183 ± 0.820	5.199 ± 1.164	<0.01
Frequency size	174.177 ± 135.557	76.024 ± 78.354	<0.01
Quantile5	1252.525 ± 788.053	1326.47 ± 831.422	0.694
Quantile10	1531.975 ± 810.426	1588.629 ± 864.324	0.766
Quantile25	2076.139 ± 732.634	2103.848 ± 848.941	0.924
Quantile50	2648.489 ± 632.203	2695.057 ± 790.953	0.831
Quantile75	3108.427 ± 591.957	3066.973 ± 713.947	0.766
Quantile90	3371.929 ± 620.665	3301.688 ± 707.829	0.617
Quantile95	3496.878 ± 607.956	3418.725 ± 701.590	0.580

Figure 3. ROC curves of the pharmacokinetic parameters (a) and histogram parameters (b) from DCE-MRI images. DCE-MRI, dynamic contrast-enhanced MRI; ROC, receiver operating characteristic.

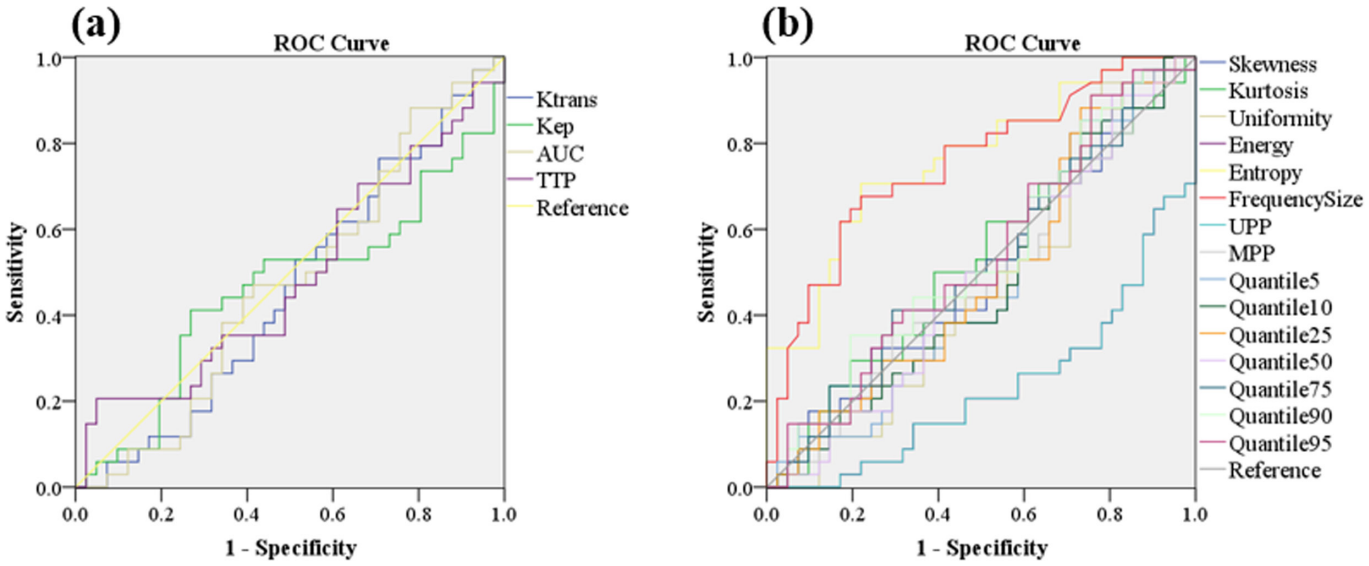

values of breast cancer in this study were consistent with those of previous research.[12,14]

Table 3 lists the promising results of the Mann–Whitney *U* test of the histogram parameters. The energy, entropy, and frequency size revealed significant differences between the patients with and without lymph node metastases ($p < 0.01$). The other histogram parameters had no significant differences ($p > 0.05$).

To identify the specificity and sensitivity of the DCE-MRI-derived quantitative parameters, we constructed the ROC curves of the pharmacokinetic and histogram parameters (Figure 3 and Table 4). The specificity and sensitivity of the pharmacokinetic parameters were lower than those of the histogram parameters in the differentiation research. However, the energy from the histogram exhibited the highest specificity and sensitivity (Figure 3 and Table 5, AUC of ROC = 0.765, maximum Jordan index = 0.486, specificity = 0.706, sensitivity = 0.780).

DISCUSSION

The occurrence of lymph node metastasis in patients with breast cancer corresponds to poor prognosis and complicated treatment.[15,16] Ultrasound is the first choice for breast tumor examination. Ultrasound-guided lymph node puncture is commonly used to identify lymph node metastasis in patients with breast cancer. MRI has also been performed to detect lymph node metastasis in breast cancer. A previous study showed that the apparent diffusion coefficient values of axillary lymph nodes can be utilized as a biomarker to differentiate between metastatic and benign axillary lymph nodes.[17] In addition to common methods, immunohistochemical examination and gene expression have been applied to reveal the correlation of patients with breast cancer and lymph node metastasis.[18,19]

The crucial aspect of lymph node metastasis among patients with breast cancer is tumor. Nothing can be explained if it is correlated with tumors, and tumor metabolism, including cytopoiesis, secretion production, and tumor cell apoptosis, can affect the function of other normal body organs. The lymph node metastasis of breast cancer is strongly related to breast tumors, and this relationship may be explained by the characteristics or heterogeneity of tumors.[20–22]

Medical imaging provides an overall assessment of tumors rather than genomics, aspiration biopsy, pathological sectioning, and immunohistochemical examination. In this research, two different analytical methods, namely, pharmacokinetic and histogram analyses, were applied to DCE-MRI to reveal the differences between breast tumors with and without lymph node metastases. Pharmacokinetic parameters reflect microstructural

Table 4. ROC indices of the pharmacokinetic parameters of the patients with breast cancer with and without lymph node metastases

Pharmacokinetic parameters	AUC of ROC	Maximum Jordan index	Sensitivity	Specificity
Ktrans	0.460	0.057	0.765	0.293
Kep	0.463	0.143	0.412	0.732
AUC-TC	0.475	0.102	0.882	0.220
TTP	0.487	0.157	0.206	0.951

AUC-TC, area under the curve of the time–concentration curve; ROC, receiver operating characteristic; TTP, time to peak.

Table 5. ROC indices of the histogram parameters of the patients with and without lymph node metastases from breast cancer

Histogram parameters	AUC of ROC	Maximum Jordan index	Sensitivity	Specificity
Skewness	0.506	0.112	0.941	0.171
Kurtosis	0.522	0.110	0.500	0.610
Uniformity	0.463	0.161	0.941	0.220
Energy	0.232	N/A	N/A	N/A
Entropy	0.765	0.486	0.706	0.780
Frequency size	0.754	0.457	0.676	0.780
Quantile5	0.473	0.121	0.853	0.268
Quantile10	0.480	0.092	0.824	0.268
Quantile25	0.494	0.151	0.882	0.268
Quantile50	0.486	0.107	0.912	0.195
Quantile75	0.520	0.119	0.412	0.707
Quantile90	0.534	0.158	0.353	0.805
Quantile95	0.537	0.156	0.912	0.244

AUC, area under the curve; ROC, receiver operating characteristic.

changes inside tumors.[7,23] In the present study, the average Ktrans, Kep, AUC-TC, and TTP of each tumor were obtained, and the comparison of the pharmacokinetic parameters between the two groups of breast cancer focused on the overall tumor differences. The results of Mann–Whitney *U* test and the ROC curves of the pharmacokinetic parameters showed no significant differences ($p > 0.05$, AUC of ROC <0.5). The evaluation of the overall tumor microvascular changes in terms of the pharmacokinetic parameters did not also reveal any difference between breast cancer with and without lymph node metastasis.

The histogram analysis of DCE-MRI was conducted on the phases where the contrast agent reached the maximum concentration based on the arterial input function obtained during pharmacokinetic analysis. This technique considerably differs from the pharmacokinetic analysis. In particular, the histogram method considers the pixel value distribution in a ROI, and uneven tumor enhancement caused by heterogeneity can be quantitatively described by histogram parameters [24,25]. The correlation between MRI enhancement and breast cancer genotyping can also be explained by histogram analysis.[9] In the present research, 13 histogram parameters were used to differentiate breast cancers with lymph node metastasis from those without lymph node metastasis. Energy exhibited the best diagnostic ability to distinguish between breast cancers with and without lymph node metastases. Energy is the quadratic sum of the pixel values in ROI and indicator of the overall enhancement degree of tumors. This result suggested that the enhancement performance of breast cancers with and without lymph node metastases differed.

The promising results of this research indicated that the difference between tumors with and without lymph node metastases can be quantitatively described by histogram parameters rather than by pharmacokinetic parameters. No sufficient number of patients could be evaluated through regression analysis or radiomics methods to preoperatively predict the lymph node status of breast cancer because of the limited number of patients. On the other hand, the size of the node means significant to the clinical treatment, since the node cannot be detected by the MR images, it was not added as an influence factor to be discussed. Nevertheless, these two points are being examined in an ongoing research.

CONCLUSION

The pharmacokinetic and histogram parameters from DCE-MRI were evaluated to identify the differences between breast cancers with and without lymph node metastasis. Histogram parameters rather than pharmacokinetic parameters indicated the diagnostic ability. To our best knowledge, this study is the first to compare the pharmacokinetic and histogram parameters of breast cancer with different lymph node statuses.

ACKNOWLEDGEMENTS

Not applicable

COMPETING INTERESTS

The authors declare that they have nocompeting interests.

CONTRIBUTORS

Xu and Zhang designed the study and drafted the manuscript, they were also responsible for the MRI scanning. Yu and Hou performed the statistical analysis and researched the literature, all authors read and approved the final version of the manuscript

ETHICS APPROVAL

This study was approved by the InstitutionalReview Board of the WeiHai Central Hospital. Written consent was obtained by all patients.

DISCLOSURE

Not applicable.

PATIENT CONSENT

Not applicable.

REFERENCES

1. Willett WC, Browne ML, Bain C, Lipnick RJ, Stampfer MJ, Rosner B, et al. Relative weight and risk of breast cancer among premenopausal women. *Am J Epidemiol* 1985; **122**: 731–40. doi: https://doi.org/10.1093/oxfordjournals.aje.a114156
2. Cuan Martínez JR, Mainero Ratchelous FE, Aguilar Gallegos IU, et al. Comparative study of clinical and pathological features of breast cancer in women with 40 years old and younger vs 70 years old and older. *Ginecología Y Obstetricia De México* 2008; **76**: 299.
3. Huang O, Wang L, Shen K, Lin H, Hu Z, Liu G, et al. Breast cancer subpopulation with high risk of internal mammary lymph nodes metastasis: analysis of 2,269 Chinese breast cancer patients treated with extended radical mastectomy. *Breast Cancer Res Treat* 2008; **107**: 379–87. doi: https://doi.org/10.1007/s10549-007-9561-4
4. Shinozaki M, Hoon DSB, Giuliano AE, Hansen NM, Wang H-J, Turner R, et al. Distinct hypermethylation profile of primary breast cancer is associated with sentinel lymph node metastasis. *Clin Cancer Res* 2005; **11**: 2156–62. doi: https://doi.org/10.1158/1078-0432.CCR-04-1810
5. Tofts PS, Kermode AG. Measurement of the blood-brain barrier permeability and leakage space using dynamic MR imaging. 1. fundamental concepts. *Magn Reson Med* 1991; **17**: 357–67. doi: https://doi.org/10.1002/mrm.1910170208
6. Pickles MD, Lowry M, Manton DJ, Turnbull LW. Prognostic value of DCE-MRI in breast cancer patients undergoing neoadjuvant chemotherapy: a comparison with traditional survival indicators. *Eur Radiol* 2015; **25**: 1097–106. doi: https://doi.org/10.1007/s00330-014-3502-5
7. Wang C-H, Yin F-F, Horton J, Chang Z. Review of treatment assessment using DCE-MRI in breast cancer radiation therapy. *World J Methodol* 2014; **4**: 46–58. doi: https://doi.org/10.5662/wjm.v4.i2.46
8. Chen LL, Zhao JN, Guo DJ. Clinical Application of ~1H-MRS Associated with DCE-MRI in Breast Cancer [J. *Chinese Computed Medical Imaging* 2008;.
9. Choi Y, Kim SH, Youn IK, Kang BJ, Park W-C, Lee A, et al. Rim sign and histogram analysis of apparent diffusion coefficient values on diffusion-weighted MRI in triple-negative breast cancer: comparison with ER-positive subtype. *PLoS One* 2017; **12**: e0177903: e0177903: . doi: https://doi.org/10.1371/journal.pone.0177903
10. Chang Y-C, Huang C-S, Liu Y-J, Chen J-H, Lu Y-S, Tseng W-YI, et al. Angiogenic response of locally advanced breast cancer to neoadjuvant chemotherapy evaluated with parametric histogram from dynamic contrast-enhanced MRI. *Phys Med Biol* 2004; **49**: 3593–602. doi: https://doi.org/10.1088/0031-9155/49/16/007
11. Cho GY, Moy L, Kim SG, Baete SH, Moccaldi M, Babb JS, et al. Evaluation of breast cancer using intravoxel incoherent motion (IVIM) histogram analysis: comparison with malignant status, histological subtype, and molecular prognostic factors. *Eur Radiol* 2016; **26**: 2547–58. doi: https://doi.org/10.1007/s00330-015-4087-3
12. Li X, Arlinghaus LR, Ayers GD, Chakravarthy AB, Abramson RG, Abramson VG, et al. DCE-MRI analysis methods for predicting the response of breast cancer to neoadjuvant chemotherapy: pilot study findings. *Magn Reson Med* 2014; **71**: 1592–602. doi: https://doi.org/10.1002/mrm.24782
13. Jiayi YU, Guo D, Luo Y, et al. Value of histogram analysis of quantitative parameters in dynamic contrastenhanced magnetic resonance imaging in diagnosis of prostate cancer[J. *Journal of Third Military Medical University* 2017;.
14. Yankeelov TE, Lepage M, Chakravarthy A, Broome EE, Niermann KJ, Kelley MC, et al. Integration of quantitative DCE-MRI and ADC mapping to monitor treatment response in human breast cancer: initial results. *Magn Reson Imaging* 2007; **25**: 1–13. doi: https://doi.org/10.1016/j.mri.2006.09.006
15. Mittra I, MacRae KD. A meta-analysis of reported correlations between prognostic factors in breast cancer: does axillary lymph node metastasis represent biology or chronology? *Eur J Cancer* 1991; **27**: 1574–83. doi: https://doi.org/10.1016/0277-5379(91)90418-D
16. Klauber-DeMore N, Ollila DW, Moore DT, Livasy C, Calvo BF, Kim HJ, et al. Size of residual lymph node metastasis after neoadjuvant chemotherapy in locally advanced breast cancer patients is prognostic. *Ann Surg Oncol* 2006; **13**: 685–91. doi: https://doi.org/10.1245/ASO.2006.03.010
17. Razek AAKA, Lattif MA, Denewer A, Farouk O, Nada N. Assessment of axillary lymph nodes in patients with breast cancer with diffusion-weighted MR imaging in combination with routine and dynamic contrast MR imaging. *Breast Cancer* 2016; **23**: 525–32. doi: https://doi.org/10.1007/s12282-015-0598-7
18. Thangarajah F, Malter W, Hamacher S, Schmidt M, Krämer S, Mallmann P, et al. Predictors of sentinel lymph node metastases in breast cancer-radioactivity and Ki-67. *Breast* 2016; **30**: 87–91. doi: https://doi.org/10.1016/j.breast.2016.09.003
19. Chen Y, Liu Y, Wang Y, Li W, Wang X, Liu X, et al. Quantification of STAT3 and VEGF expression for molecular diagnosis of lymph node metastasis in breast cancer. *Medicine* 2017; **96**: e8488: e8488: . doi: https://doi.org/10.1097/MD.0000000000008488
20. Liu L-J, Shu X-J, Zhen H-Y, Qiu X-D, Deng H, Zhou H-Y, et al. Correlation of histological heterogeneity and lymph node metastasis in gastric adenocarcinoma. *World Chinese Journal of Digestology* 2004; **12**: 1273. doi: https://doi.org/10.11569/wcjd.v12.i6.1273
21. Torres L, Ribeiro FR, Pandis N, Andersen JA, Heim S, Teixeira MR, et al. Intratumor genomic heterogeneity in breast cancer with clonal divergence between primary carcinomas and lymph node metastases. *Breast Cancer Res Treat* 2007; **102**: 143–55. doi: https://doi.org/10.1007/s10549-006-9317-6
22. Ellsworth RE, Toro AL, Blackburn HL, Decewicz A, Deyarmin B, Mamula KA, et al. Molecular heterogeneity in primary breast carcinomas and axillary lymph node metastases assessed by genomic fingerprinting analysis. *Cancer Growth Metastasis* 2015; **8**: CGM.S29490–24. doi: https://doi.org/10.4137/CGM.S29490
23. Tofts PS, Kermode AG. Measurement of the blood-brain barrier permeability and leakage space using dynamic MR imaging. 1. fundamental concepts. *Magn Reson Med* 1991; **17**: 357–67. doi: https://doi.org/10.1002/mrm.1910170208

24. Lee S, Choi SH, Ryoo I, Yoon TJ, Kim TM, Lee S-H, et al. Evaluation of the microenvironmental heterogeneity in high-grade gliomas with IDH1/2 gene mutation using histogram analysis of diffusion-weighted imaging and dynamic-susceptibility contrast perfusion imaging. *J Neurooncol* 2015; **121**: 141–50. doi: https://doi.org/10.1007/s11060-014-1614-z
25. Wang S, Kim S, Zhang Y, Wang L, Lee EB, Syre P, et al. Determination of grade and subtype of meningiomas by using histogram analysis of diffusion-tensor imaging metrics. *Radiology* 2012; **262**: 584–92. doi: https://doi.org/10.1148/radiol.11110576